$W\gamma$ and $Z\gamma$ production at the LHC in NNLO QCD

Stefan Kallweit[1]

based on work with: M. Grazzini, D. Rathlev and A. Torre
Phys. Lett. B731 (2014) 204-207 [arXiv:1309.7000 [hep-ph]]

and with: M. Grazzini and D. Rathlev
arXiv:1504.01330 [hep-ph] (accepted for publication in JHEP)

[1]University of Mainz

June 15–19, 2015, Radcor-Loopfest 2015
University of California, Los Angeles (UCLA)

Outline

1. Introduction

2. Calculation of NNLO QCD cross sections with q_{T} subtraction
   - Idea of q_{T} subtraction method
   - Technical details and implementation

3. Numerical results at NNLO QCD and comparison to ATLAS data
   - Inclusive and differential cross sections for $\mathrm{pp}\,(\to \mathrm{Z}\gamma) \to \mathrm{l}^-\mathrm{l}^+\gamma + \mathrm{X}$
   - Inclusive and differential cross sections for $\mathrm{pp}\,(\to \mathrm{Z}\gamma) \to \nu_\mathrm{l}\bar{\nu}_\mathrm{l}\gamma + \mathrm{X}$
   - Inclusive and differential cross sections for $\mathrm{pp}\,(\to \mathrm{W}\gamma) \to \mathrm{l}\nu_\mathrm{l}\gamma + \mathrm{X}$
   - Comparison between $\mathrm{Z}\gamma$ and $\mathrm{W}\gamma$ results

4. Conclusions & Outlook

Importance of going beyond NLO in QCD in Vγ production

Fully exclusive NNLO QCD calculations desirable for several reasons

- Experimental accuracy has significantly increased.
- A reduction of the unphysical dependence on factorization and renormalization scales — and in particular reliability of the remaining scale-variation uncertainty as an estimate for missing higher orders — is expected at NNLO.
  - In many process classes, all partonic channels are included only from NNLO on.
  - In some phase-space regions, NLO is the first non-vanishing order.
  - Jets are treated more realistically.

On the same expected order of magnitude (by naive counting of coupling constants), NLO EW corrections should also be taken into account.

Importance of Vγ production (with leptonic decays) at NNLO QCD

- Important Standard Model test $\rightarrow$ trilinear gauge-boson couplings.
- Background for Higgs analyses and BSM searches.
- Some moderate excesses ($\approx 2\sigma$) in the experimental data compared to NLO predicion (e.g. Wγ in ATLAS analysis at 7 TeV).

Sketchy presentation of the q_T subtraction method

Consider the production of a **colourless final state F** via $\mathbf{q\bar{q} \to F}$ or $\mathbf{gg \to F}$:

$$\mathrm{d}\sigma_{\mathrm{F}}^{\mathrm{(N)NLO}}\Big|_{q_T \neq 0} = \mathrm{d}\sigma_{\mathrm{F+jet}}^{\mathrm{(N)LO}},$$

where q_T refers to the transverse momentum of the colourless system F.
[Catani, Grazzini (2007)]

- $\mathrm{d}\sigma_{\mathrm{F}}^{\mathrm{(N)NLO}}\Big|_{q_T \neq 0}$ is singular for $q_T \to 0$, but the limiting behaviour is known from transverse momentum resummation.
  [Bozzi, Catani, de Florian, Grazzini (2006)]

- Define a counterterm,

$$\mathrm{d}\sigma^{\mathrm{CT}} = \Sigma(q_T/Q) \otimes \mathrm{d}\sigma^{\mathrm{LO}}, \quad Q \equiv m_{\mathrm{F}},$$

  which has the same limiting behaviour for $q_T \to 0$.

- Add the $q_T = 0$ piece to obtain the full result:

$$\boldsymbol{\mathrm{d}\sigma_{\mathrm{F}}^{\mathrm{(N)NLO}} = \mathcal{H}_{\mathrm{F}}^{\mathrm{(N)NLO}} \otimes \mathrm{d}\sigma^{\mathrm{LO}} + \left[\mathrm{d}\sigma_{\mathrm{F+jet}}^{\mathrm{(N)LO}} - \Sigma \otimes \mathrm{d}\sigma^{\mathrm{LO}}\right]}$$

Ingredients of the $q_{\rm T}$ subtraction method

$$\mathrm{d}\sigma_{\rm F}^{\rm (N)NLO} = \mathcal{H}_{\rm F}^{\rm (N)NLO} \otimes \mathrm{d}\sigma^{\rm LO} + \left[\mathrm{d}\sigma_{\rm F+jet}^{\rm (N)LO} - \Sigma \otimes \mathrm{d}\sigma^{\rm LO}\right]$$

- The hard–virtual coefficients,

$$\mathcal{H}_{\rm F} = \underbrace{1}_{\substack{\text{tree-level}\\ \text{amplitude}}} + \underbrace{\left(\frac{\alpha_S}{\pi}\right)\mathcal{H}^{\rm F(1)}}_{\substack{\text{contains (finite)}\\ \text{1-loop amplitude}}} + \underbrace{\left(\frac{\alpha_S}{\pi}\right)^2\mathcal{H}^{\rm F(2)}}_{\substack{\text{contains (finite)}\\ \text{2-loop amplitude}}} + \ldots,$$

  are known up to 2-loop order by means of a process-independent extraction procedure, starting from the all-order virtual amplitude of the specific process.
  [Catani, Cieri, de Florian, Ferrera, Grazzini (2013)]

- $\mathrm{d}\sigma_{\rm F+jet}^{\rm NLO}$ can be treated by well-known local NLO subtraction techniques.

- The counterterm

$$\Sigma(q_{\rm T}/Q) = \left(\frac{\alpha_S}{\pi}\right)\Sigma^{(1)}(q_{\rm T}/Q) + \left(\frac{\alpha_S}{\pi}\right)^2\Sigma^{(2)}(q_{\rm T}/Q) + \ldots$$

  is universal (differs for $\mathrm{q\bar{q}} \to \mathrm{F}$ and $\mathrm{gg} \to \mathrm{F}$, trivial process dependence), and the coefficients are known (up to 2-loop order).
  [Bozzi, Catani, de Florian, Grazzini (2006)]

NNLO QCD cross section via q_{T} subtraction

Schematic formula for the NNLO cross section

$$\sigma^{\mathrm{NNLO}} = \underbrace{\underbrace{\int_{m+2} d\sigma^{RR}}_{\text{double-real}} + \underbrace{\int_{m+1} d\sigma^{RV}}_{\text{real–virtual}} + \underbrace{\int_0^1 dz \int_{m+1} d\sigma^{RC}}_{\text{real–collinear}}}$$

$= \sigma^{\mathrm{NLO}}_{F+jet}$ $\Rightarrow$ at $q_{\mathrm{T}} \neq 0$ calculable via NLO subtraction, but divergent for $q_{\mathrm{T}} \to 0 \Rightarrow \mathrm{cut}_{q_{\mathrm{T}}/q}$

$$+ \underbrace{\int_m d\sigma^{VV}}_{\text{double-virtual}} + \underbrace{\int_0^1 dz \int_m d\sigma^{VC}}_{\text{virtual–collinear}} + \underbrace{\int_0^1 dz_1 \int_0^1 dz_2 \int_m d\sigma^{CC}}_{\text{double-collinear}}$$

$$= \sigma^{\mathrm{NLO}}_{F+jet}\Big|_{q_{\mathrm{T}}/q \, > \, \mathrm{cut}_{q_{\mathrm{T}}/q}}$$

$$+ \underbrace{\sigma^{\mathrm{NLO}}_{F+jet}\Big|_{q_{\mathrm{T}}/q \, \leq \, \mathrm{cut}_{q_{\mathrm{T}}/q}}}_{\text{approximated by results known from } q_{\mathrm{T}} \text{ resummation}} + \underbrace{\int_m d\sigma^{VV} + \int_0^1 dz \int_m d\sigma^{VC} + \int_0^1 dz_1 \int_0^1 dz_2 \int_m d\sigma^{CC}}_{\text{identified with corresponding terms in } q_{\mathrm{T}} \text{ resummation}}$$

NNLO QCD cross section via q_T subtraction

Schematic formula for the NNLO cross section

$$\sigma^{\mathrm{NNLO}} = \underbrace{\left[\int_{m+2} d\sigma^{RRA} + \int_{m+1} d\sigma^{RVA} + \int_0^1 dz \int_{m+1} d\sigma^{RCA}\right]\Bigg|_{q_\mathrm{T}/q\,>\,\mathrm{cut}_{q_\mathrm{T}/q}}}_{=\,\sigma^{\mathrm{NLO}}_{F+jet}\big|_{q_\mathrm{T}/q\,>\,\mathrm{cut}_{q_\mathrm{T}/q}}}$$

$\Rightarrow$ finite, but dependence on $\mathrm{cut}_{q_\mathrm{T}/q}$

$$+\left(\frac{\alpha_S}{\pi}\right)^2 \mathcal{H}^{F(2)} \otimes \sigma_{\mathrm{LO}}$$

- no $\mathrm{cut}_{q_\mathrm{T}/q}$ dependence,
- contains (finite) 2-loop part.

$$+\left(\frac{\alpha_S}{\pi}\right)^2 \int_{\mathrm{cut}_{q_\mathrm{T}/q}}^{\infty} d(q_\mathrm{T}/q)\Sigma^{(2)}(q_\mathrm{T}/q) \otimes \sigma_{\mathrm{LO}}$$

- cancels $\mathrm{cut}_{q_\mathrm{T}/q}$ dependence,
- contains (finite) 1-loop part,
- assigned to Born phase-space.

All relevant ingredients from q_T resummation ($\mathcal{H}^{F(i)}$, $\Sigma^{(i)}(q_\mathrm{T}/q)$ for $i \leq 2$) are known.

$\hookrightarrow$ **Direct implementation into a Monte Carlo integrator feasible.**

Numerical realization of the calculation

Realized within the fully automated NLO (QCD+EW) Monte Carlo framework
MUNICH (MUlti-chaNnel Integrator at Swiss (CH) precision) [SK]

- Applicable for arbitrary Standard Model processes (including partonic bookkeeping).
- Phase-space integration by highly efficient multi-channel Monte Carlo techniques
  ↪ Additional MC channels based on dipole kinematics constructed at runtime.
- OpenLoops interface, automatized implementation of dipole subtraction, etc.
- Simultaneous calculation for different scale choices and variations.

Extension to automated (q_T subtraction) NNLO QCD framework [Grazzini, SK, Rathlev]

- Process-independent construction of $\mathrm{cut}_{q_T/q}$-dependent counterterms $\Sigma^{(1,2)}$.
- Process-independent extraction procedure for hard coefficients $\mathcal{H}^{(1,2)}$.
- NLO calculation for F+jet with finite $\mathrm{cut}_{q_T/q}$ already available in Munich.
- Importance sampling performed on top of multi-channel approach
  ↪ improved efficiency and reliability in particular for low $\mathrm{cut}_{q_T/q}$ values.
- Simultaneous evaluation of observables for different values of the regulator $\mathrm{cut}_{q_T/q}$
  ↪ allows for monitoring of $\mathrm{cut}_{q_T/q}$ and for extrapolation $\mathrm{cut}_{q_T/q} \to 0$.

Numerical stability and dependence on $\mathrm{cut}_{q_T/q}$

q_T subtraction at NLO

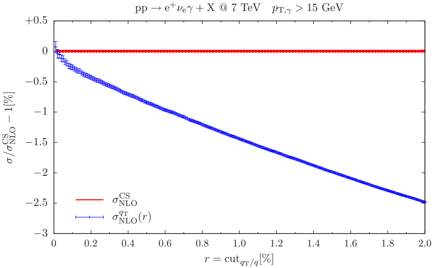

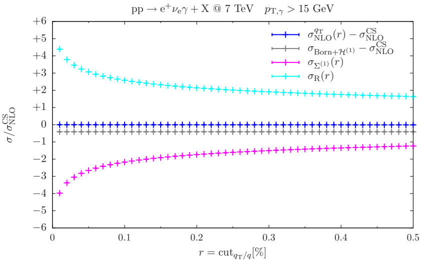

q_T subtraction at NNLO

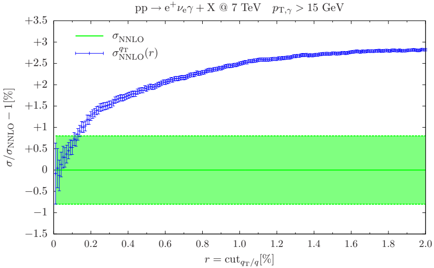

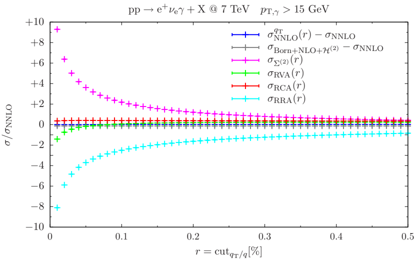

Photon isolation

Two contributions to photon production

- Direct production in the hard process,
- Non-perturbative fragmentation of a hard parton.

Different approaches to define isolated photons

- Naive ansatz: forbid any partons inside a fixed cone around the photon.
  ↪ Not infrared safe beyond LO QCD as soft gluons inside the cone are forbidden.
- Hard cone isolation (experimentally preferred)

$$\sum_{\delta'<\delta_0} E_{\mathrm{had,T}}(\delta') \quad \leq \quad \varepsilon_\gamma E_{\gamma,\mathrm{T}}, \qquad\qquad \delta_{i\gamma} = \sqrt{(\eta_i - \eta_\gamma)^2 + (\phi_i - \phi_\gamma)^2}$$

  ↪ Only infrared safe if combined with fragmentation contribution (due to quark–photon collinear singularity).
- **Smooth cone isolation** [Frixione (1998)]

$$\sum_{\delta'<\delta} E_{\mathrm{had,T}}(\delta') \quad \leq \quad \varepsilon_\gamma E_{\gamma,\mathrm{T}} \left(\frac{1-\cos(\delta)}{1-\cos(\delta_0)}\right)^n \quad \forall \quad \delta \leq \delta_0$$

  ↪ Smooth cone isolation eliminates fragmentation contribution completely.

Technical ingredients of the calculation

Scattering amplitudes up to 1-loop with OpenLoops [Cascioli, Maierhöfer, Pozzorini (2011); Cascioli, Lindert, Maierhöfer, Pozzorini (2014)]

- Tree, one-loop and real-emission amplitudes (including colour/helicity correlations)
- Provides also finite (1-loop)-squared amplitudes (not only)
- Fully automated for NLO (QCD+EW) for any SM process
- Compact and fast numerical code

Tensor reduction by means of the Collier library [Denner, Dittmaier, Hofer (2014)]

- Numerically stable Denner–Dittmaier reduction methods [Denner, Dittmaier (2002 & 2005)]
- Scalar integrals with complex masses [Denner, Dittmaier (2010)]

Rescue system by quad-precision CutTools for critical points [Ossola, Papadopoulos, Pittau (2008)]

- Scalar integrals from OneLOop [van Hameren, Papadopoulos, Pittau (2009)]; van Hameren (2010)]

2-loop amplitudes from analytic results [Matsuura, van der Marck, van Neerven (1989); Gehrmann, Tancredi (2011)]

Mediation of IR divergences between phase-spaces

- Dipole subtraction for massless particles in NLO-like parts [Catani, Seymour (1993)]
- q_T subtraction for dealing with the remaining singularities [Catani, Grazzini (2007)]

Numerical results for $\mathrm{pp} \to \mathrm{Z}\gamma \to \mathrm{l}^-\mathrm{l}^+\gamma + \mathrm{X}$ at NNLO QCD

Setup adapted to the ATLAS analysis @ 7 TeV

[ATLAS collaboration (2013)]

Leptons	$p_\mathrm{T}^\ell > 25\,\mathrm{GeV}$ $\lvert\eta^\ell\rvert < 2.47$
Photon	$p_\mathrm{T}^\gamma > 15\,\mathrm{GeV}$ (soft p_T^γ cut) or $p_\mathrm{T}^\gamma > 40\,\mathrm{GeV}$ (hard p_T^γ cut) $\lvert\eta^\gamma\rvert < 2.37$ Frixione isolation with $\varepsilon_\gamma = 0.5$, $R = 0.4$, $n = 1$
Jets	anti-k_T algorithm with $D = 0.4$ $p_\mathrm{T}^\mathrm{jet} > 30\,\mathrm{GeV}$ $\lvert\eta^\mathrm{jet}\rvert < 4.4$ $N_\mathrm{jet} \geq 0$ (inclusive) or $N_\mathrm{jet} = 0$ (exclusive)
Separation	$m_{\ell^+\ell^-} > 40\,\mathrm{GeV}$ $\Delta R(\ell,\gamma) > 0.7$ $\Delta R(\ell/\gamma,\mathrm{jet}) > 0.3$

LO diagrams

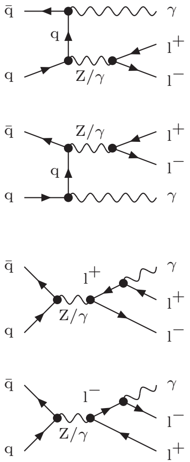

Integrated cross sections (LHC @ 7 TeV, ATLAS setups)

(central scale: $\mu_\mathrm{R} = \mu_\mathrm{F} = \sqrt{m_\mathrm{Z}^2 + p_{\gamma,\mathrm{T}}^2}$, independent μ_R, μ_F variation by factor 2):

$p_{\mathrm{T,cut}}^{\gamma}$	N_jet	σ_LO [pb]	σ_NLO [pb]	σ_NNLO [pb]	σ_ATLAS [pb]
soft	$N_\mathrm{jet} \geq 0$	$0.8149\,^{+8.0\%}_{-9.3\%}$	$1.222\,^{+4.2\%}_{-5.3\%}$	$1.320\,^{+1.3\%}_{-2.3\%}$	$1.31\ \pm0.02\ (\mathrm{stat})\ \pm0.11\ (\mathrm{syst})\ \pm0.05\ (\mathrm{lumi})$
soft	$N_\mathrm{jet} = 0$	$0.8149\,^{+8.0\%}_{-9.3\%}$	$1.031\,^{+2.7\%}_{-4.3\%}$	$1.059\,^{+0.7\%}_{-1.4\%}$	$1.05\ \pm0.02\ (\mathrm{stat})\ \pm0.10\ (\mathrm{syst})\ \pm0.04\ (\mathrm{lumi})$
hard	$N_\mathrm{jet} \geq 0$	$0.07361\,^{+3.4\%}_{-4.5\%}$	$0.1320\,^{+4.2\%}_{-4.0\%}$	$0.1543\,^{+3.1\%}_{-2.8\%}$	

- Reasonable agreement between experimental result and theory prediction in the soft setup, both at NLO and NNLO (only small NNLO corrections).
- Scale variations in exclusive setup most likely underestimate the remaining theoretical uncertainties (no jet-veto resummation).
- Loop-induced gg contribution turns out to be very small.
  - $\hookrightarrow$ $\lesssim$ 6% of $\mathcal{O}(\alpha_\mathrm{s}^2)$ correction, $\lesssim$ 0.5% of inclusive NNLO result with soft p_T^γ cut,
    $\lesssim$ 10% of $\mathcal{O}(\alpha_\mathrm{s}^2)$ correction, $\lesssim$ 1.5% of inclusive NNLO result with hard p_T^γ cut.

Distribution in $m_{\mathrm{l}^-\mathrm{l}^+\gamma}$ (LHC @ 7 TeV, ATLAS soft vs. hard setup)

$p_{\mathrm{T,cut}}^{\gamma}$	N_{jet}	$\sigma_{\mathrm{NLO}}/\sigma_{\mathrm{LO}}$	$\sigma_{\mathrm{NNLO}}/\sigma_{\mathrm{NLO}}$
soft	$N_{\mathrm{jet}} \geq 0$	+50%	+8%
	$N_{\mathrm{jet}} = 0$	+27%	+3%
hard	$N_{\mathrm{jet}} \geq 0$	+79%	+17%

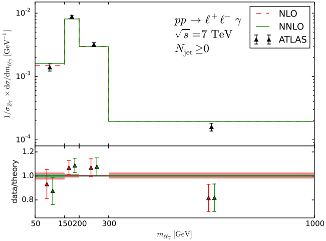

- Implicit LO phase-space restrictions:
  $m_{\ell\ell\gamma} \approx 66\,\mathrm{GeV}$ (soft) vs. $m_{\ell\ell\gamma} \approx 97\,\mathrm{GeV}$ (hard)

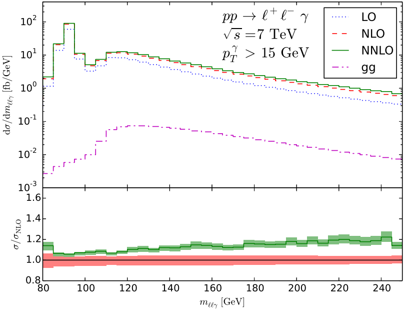

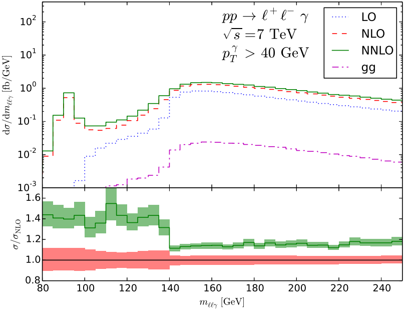

Data comparison: p_T^γ (LHC @ 7 TeV, ATLAS soft setup)

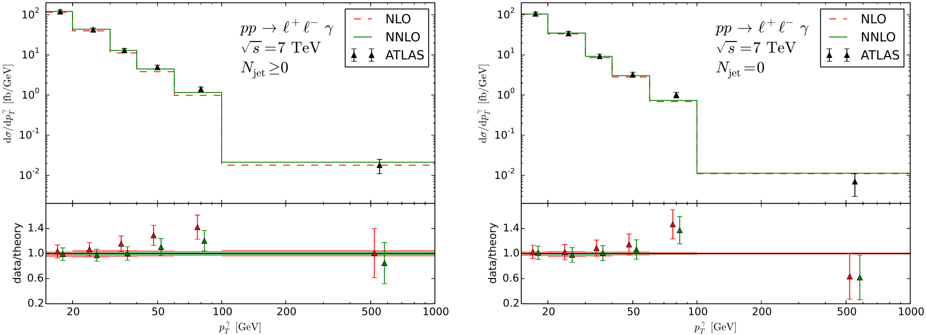

- Quite good agreement between data and theory at both NLO and NNLO.
  - ↪ Slight tension in some bins at NLO released by NNLO corrections.
- Theory error in exclusive prediction probably underestimated by naive scale variation.
- No electroweak corrections included.
  - ↪ Possibly large (negative) effects to be expected in high-p_T region.

Numerical results for $\mathrm{pp} \to \mathrm{Z}\gamma \to \nu\bar{\nu}\gamma + \mathrm{X}$ at NNLO QCD

Setup adapted to the ATLAS analysis @ 7 TeV

[ATLAS collaboration (2013)]

Neutrinos	$p_{\mathrm{T}}^{\nu\bar{\nu}} > 90\,\mathrm{GeV}$
Photon	$p_{\mathrm{T}}^{\gamma} > 100\,\mathrm{GeV}$
	$\lvert\eta^{\gamma}\rvert < 2.37$
	Frixione isolation with $\varepsilon_{\gamma} = 0.5$, $R = 0.4$, $n = 1$
Jets	$p_{\mathrm{T}}^{\mathrm{jet}} > 30\,\mathrm{GeV}$
	$\lvert\eta^{\mathrm{jet}}\rvert < 4.4$
	$N_{\mathrm{jet}} \geq 0$ (inclusive) or $N_{\mathrm{jet}} = 0$ (exclusive)
Separation	$\Delta R(\gamma, \mathrm{jet}) > 0.3$

LO diagrams

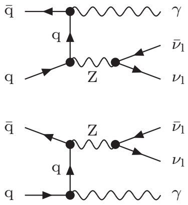

Integrated cross sections (LHC @ 7 TeV, ATLAS setups)

(central scale: $\mu_\mathrm{R} = \mu_\mathrm{F} = \sqrt{m_\mathrm{Z}^2 + p_{\gamma,\mathrm{T}}^2}$, independent μ_R, μ_F variation by factor 2):

N_jet	σ_LO [pb]	σ_NLO [pb]	σ_NNLO [pb]	σ_ATLAS [pb]
$N_\mathrm{jet} \geq 0$	$78.81\,^{+0.3\%}_{-0.9\%}$	$123.69\,^{+4.1\%}_{-3.1\%}$	$138.03\,^{+2.5\%}_{-2.3\%}$	$133\ \pm13\ \mathrm{(stat)}\ \pm20\ \mathrm{(syst)}\ \pm\ 5\ \mathrm{(lumi)}$
$N_\mathrm{jet} = 0$		$88.08\,^{+1.2\%}_{-1.3\%}$	$86.55\,^{+1.0\%}_{-0.9\%}$	$116\ \pm10\ \mathrm{(stat)}\ \pm13\ \mathrm{(syst)}\ \pm\ 4\ \mathrm{(lumi)}$

- Results summed over 3 neutrino generations.
- Inclusive cross section in reasonable agreement, both at NLO and at NNLO (limited by experimental accuracy).
- Significant discrepancy for $N_\mathrm{jet} = 0$ with respect to ATLAS measurement.
  - ↪ Can be attributed to hadronization effects: ATLAS applies $\mathcal{O}(30\%)$ correction factor to parton-level prediction. (sizable effect, as $\mathrm{Z} \to \nu\nu$ is only identified by photon and additional radiation)
- Loop-induced gg contribution turns out to be relatively small
  - ↪ $\lesssim 14\%$ of $\mathcal{O}(\alpha_\mathrm{s}^2)$ correction, $\lesssim 1.5\%$ of inclusive NNLO result.

Distribution in $m_{\mathrm{T}}^{\nu\nu\gamma}$ (LHC @ 7 TeV, ATLAS setup)

N_{jet}	$\sigma_{\mathrm{NLO}}/\sigma_{\mathrm{LO}}$	$\sigma_{\mathrm{NNLO}}/\sigma_{\mathrm{NLO}}$
$N_{\mathrm{jet}} \geq 0$	$+57\%$	$+12\%$
$N_{\mathrm{jet}} = 0$	$+12\%$	-2%

$$m_{\mathrm{T}}^{\nu\nu\gamma} = \sqrt{\left(\left|\vec{p}_T^{\,\gamma}\right| + E_T^{\mathrm{miss}}\right)^2 - \left|\vec{p}_T^{\,\gamma} + \vec{E}_T^{\mathrm{miss}}\right|^2}$$

- Implicit LO phase-space restriction $m_{\mathrm{T}}^{\nu\nu\gamma} \approx 200\,\mathrm{GeV}$ is overcome by real emission for $N_{\mathrm{jet}} \geq 0$ at NLO and NNLO.
- For $N_{\mathrm{jet}} = 0$ (allowing for 1/2 jets with $p_{\mathrm{T}}^{\mathrm{jet}} < 30\,\mathrm{GeV}$), it is slightly loosened to $m_{\mathrm{T}}^{\nu\nu\gamma} \approx 187\,\mathrm{GeV}$ (NLO) and $m_{\mathrm{T}}^{\nu\nu\gamma} \approx 175\,\mathrm{GeV}$ (NNLO), respectively.

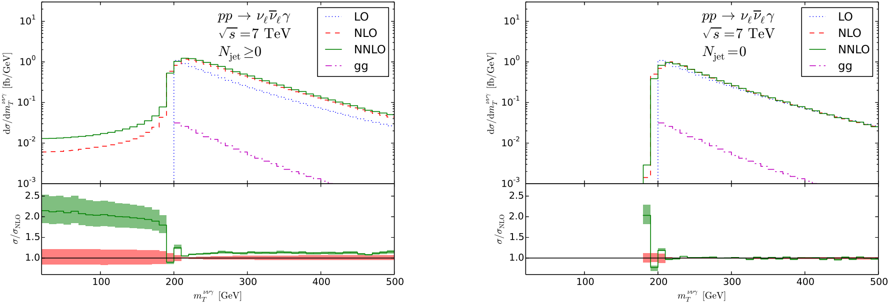

Data comparison: p_T^γ and $p_\mathrm{T}^\mathrm{miss}$ (LHC @ 7 TeV, ATLAS setup)

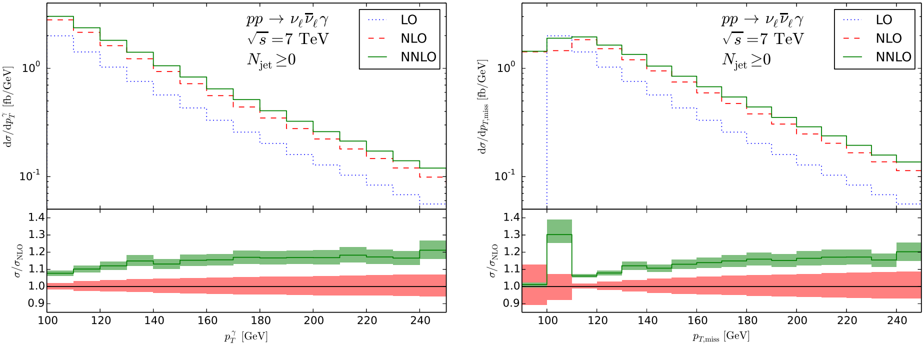

- Both distributions are obviously identical for Born kinematics.
  - ↪ Difference results purely from real-radiation corrections.
- Perturbative instability around $p_{T,\mathrm{miss}} \approx 100$ GeV, originating from incomplete cancellation of virtual and real corrections close to the phase-space boundary.
  - ↪ integrable singularity without effect on the inclusive cross section. (resummed computation needed for reliable differential prediction)

Numerical results for $\mathrm{pp} \to \mathrm{W}\gamma \to \mathrm{l}\nu\gamma + \mathrm{X}$ at NNLO QCD

Setup adapted to the ATLAS analysis @ 7 TeV

[ATLAS collaboration (2013)]

Lepton	$p_\mathrm{T}^\ell > 25\,\mathrm{GeV}$ $\lvert\eta\rvert < 2.47$
Neutrino	$p_\mathrm{T}^\nu > 35\,\mathrm{GeV}$
Photon	$p_\mathrm{T}^\gamma > 15\,\mathrm{GeV}$ (soft p_T^γ cut) or $p_\mathrm{T}^\gamma > 40\,\mathrm{GeV}$ (hard p_T^γ cut) $\lvert\eta^\gamma\rvert < 2.37$ Frixione isolation with $\varepsilon_\gamma = 0.5$, $R = 0.4$, $n = 1$
Jets	anti-k_T algorithm with $D = 0.4$ $p_\mathrm{T}^\mathrm{jet} > 30\,\mathrm{GeV}$ $\lvert\eta^\mathrm{jet}\rvert < 4.4$ $N_\mathrm{jet} \geq 0$ (inclusive) or $N_\mathrm{jet} = 0$ (exclusive)
Separation	$\Delta R(\ell, \gamma) > 0.7$ $\Delta R(\ell/\gamma, \mathrm{jet}) > 0.3$

LO diagrams

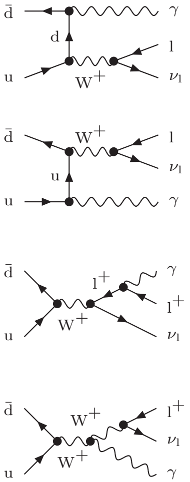

Integrated cross sections (LHC @ 7 TeV, ATLAS setups)

(central scale: $\mu_\mathrm{R} = \mu_\mathrm{F} = \sqrt{m_\mathrm{W}^2 + p_{\gamma,\mathrm{T}}^2}$, independent μ_R, μ_F variation by factor 2):

$p_{\mathrm{T,cut}}^{\gamma}$	N_jet	σ_LO [pb]	σ_NLO [pb]	σ_NNLO [pb]	σ_ATLAS [pb]
soft	$N_\mathrm{jet} \geq 0$	$0.8726\,^{+6.8\%}_{-8.1\%}$	$2.058\,^{+6.8\%}_{-6.8\%}$	$2.453\,^{+4.1\%}_{-4.1\%}$	2.77 ± 0.03 (stat) ± 0.33 (syst) ± 0.14 (lumi)
	$N_\mathrm{jet} = 0$		$1.395\,^{+5.2\%}_{-5.8\%}$	$1.493\,^{+1.7\%}_{-2.7\%}$	1.76 ± 0.03 (stat) ± 0.21 (syst) ± 0.08 (lumi)
hard	$N_\mathrm{jet} \geq 0$	$0.1158\,^{+2.6\%}_{-3.7\%}$	$0.3959\,^{+9.0\%}_{-7.3\%}$	$0.4971\,^{+5.3\%}_{-4.7\%}$	

- Results summed over $\mathrm{W}^+\gamma$ and $\mathrm{W}^-\gamma$ (as in experimental analyses).
- Large NLO corrections can be explained by breaking of "radiation zero".
- Inclusive cross section shows an $\approx 2\sigma$ excess with respect to NLO prediction.
  ↪ Reduced to well below 1σ by including the NNLO correction.
- Excess in the measured exclusive cross section is slightly reduced from $\approx 1.6\sigma$ to $\approx 1.2\sigma$ when going from NLO to NNLO.

Distribution in $m_\mathrm{T}^{\ell\nu\gamma}$ (LHC @ 7 TeV, ATLAS soft vs. hard setup)

$p_{\mathrm{T,cut}}^{\gamma}$	N_jet	$\sigma_\mathrm{NLO}/\sigma_\mathrm{LO}$	$\sigma_\mathrm{NNLO}/\sigma_\mathrm{NLO}$
soft	$N_\mathrm{jet} \geq 0$	+136%	+19%
	$N_\mathrm{jet} = 0$	+60%	+7%
hard	$N_\mathrm{jet} \geq 0$	+242%	+26%

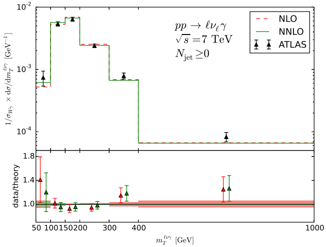

- Implicit LO phase-space restrictions:
  $m_\mathrm{T}^{\ell\nu\gamma} \approx 75\,\mathrm{GeV}$ (soft) vs. $m_\mathrm{T}^{\ell\nu\gamma} \approx 100\,\mathrm{GeV}$ (hard)

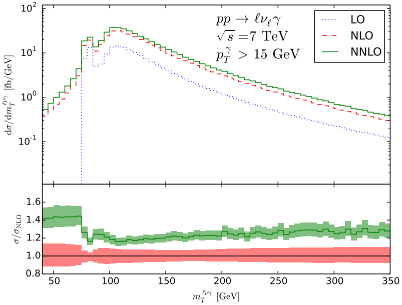

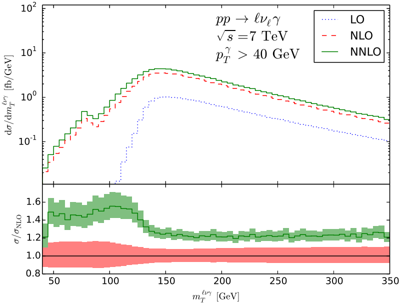

Data comparison: p_T^γ (LHC @ 7 TeV, ATLAS setup, $p_{\mathrm{T},\gamma} > 15\,\mathrm{GeV}$)

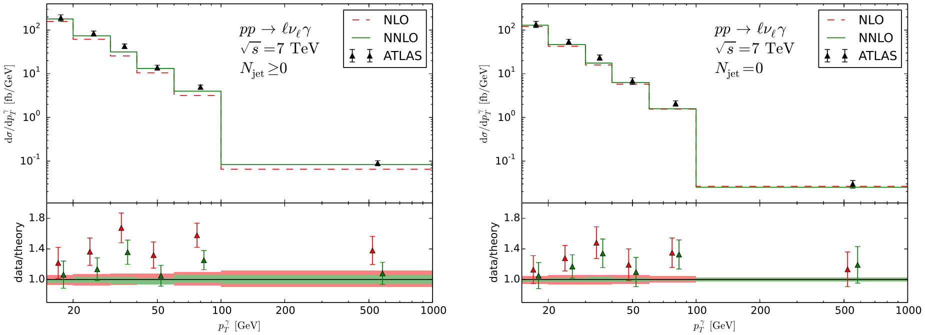

- Agreement between data and theory is significantly improved when including NNLO corrections as compared to NLO prediction, in particular without jet veto (mild improvement also for $N_\mathrm{jet} = 0$).
- Theory error in exclusive prediction probably underestimated by naive scale variation.
- No electroweak corrections (with possibly large impact in high-p_T region) included.
  - ↪ EW corrections are known and could be combined. [Denner, Dittmaier, Hecht, Pasold (2014)]

Comparison between $\mathrm{Z}\gamma$ and $\mathrm{W}\gamma$ results

Considerably larger K factors in Wγ than in Zγ

process	$p_{\mathrm{T,cut}}^{\gamma}$	N_{jet}	$\frac{\sigma_{\mathrm{NLO}}}{\sigma_{\mathrm{LO}}}$	$\frac{\sigma_{\mathrm{NNLO}}}{\sigma_{\mathrm{NLO}}}$
$Z\gamma$ $W\gamma$	soft	$N_{\mathrm{jet}} \geq 0$	+50% +136%	+8% +19%
$Z\gamma$ $W\gamma$	soft	$N_{\mathrm{jet}} = 0$	+27% +60%	+3% +7%
$Z\gamma$ $W\gamma$	hard	$N_{\mathrm{jet}} \geq 0$	+79% +242%	+17% +26%

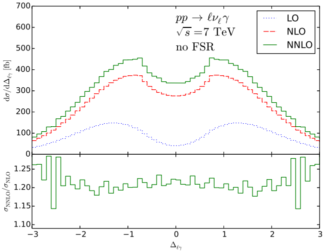

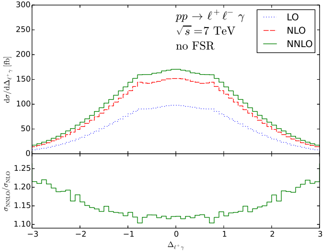

Explanation: **Breaking of radiation zero beyond LO**

- $\mathrm{u\bar{d}/d\bar{u}} \to \mathrm{W}^{\pm}\gamma$ amplitudes vanish at $\cos\theta_{\mathrm{q}\gamma,\mathrm{CMS}} = \mp 1/3$. [Mikaelian/Samuel/Sahdev (1979)]
- Radiation zero leads to a dip at $\Delta \mathrm{y}_{\mathrm{l}\gamma} = 0$ in pp collisions. [Baur/Errede/Landsberg (1994)]

  $\hookrightarrow$ Dip filled by higher-order corrections.

Conclusions & Outlook

Conclusions

- Widely automated framework to perform fully differential NNLO QCD computations for the production of colourless final states, based on MUNICH and q_{T} subtraction, making use of OPENLOOPS and dedicated two-loop amplitudes.
- Fully differential NNLO QCD results for $\mathrm{pp} \to \mathrm{V}\gamma + \mathrm{X}$ for all leptonic decay channels.
  - Full leptonic decays with spin correlations and off-shell effects included.
  - NNLO corrections typically not covered by NLO scale uncertainties.
  - NNLO and NLO corrections for $\mathrm{W}\gamma$ much larger than for $\mathrm{Z}\gamma$ (radiation zero).
  - Loop-induced gg contributions turn out to be very small ($< 15\%$ of NNLO).

Outlook

- More phenomenological studies on $\mathrm{pp} \to \mathrm{V}\gamma + \mathrm{X}$, in particular when analysis details and data at 8 TeV are available (both ATLAS and CMS).
- Combination with NLO EW corrections (sizable in high-p_{T} regions).
- Simultaneous calculation of pdf uncertainties (estimated to be at a few per cent).
- Two-loop helicity amplitudes for VV' with two different masses are available now.
  ↪ Fiducial cross sections for off-shell $\mathrm{W}^+\mathrm{W}^-$, $\mathrm{W}^\pm\mathrm{Z}$ and ZZ production with full leptonic decays at NNLO QCD will be available soon within this framework.

Extended Outlook

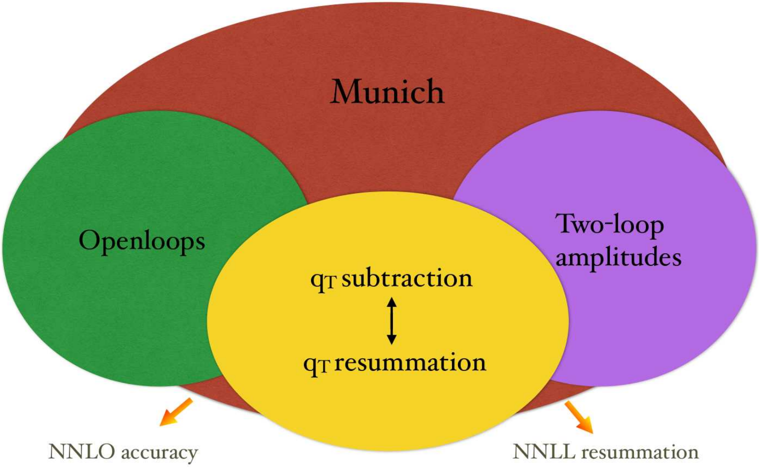

Backup

Backup slides

Scale variation (LHC @ 7 TeV, ATLAS setup, $p_{\mathrm{T},\gamma} > 15\,\mathrm{GeV}$)

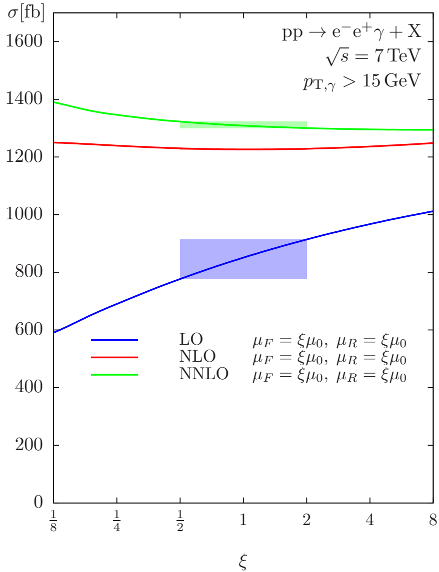

- (Central) scale choice:
  $\mu_\mathrm{R} = \mu_\mathrm{F} = \mu_0 \equiv \sqrt{m_\mathrm{Z}^2 + p_{\gamma,\mathrm{T}}^2}$.
- Scale variation essentially disappears at NLO and NNLO if variation with $\mu_\mathrm{F} = \mu_\mathrm{R}$ is considered.

  $\hookrightarrow$ accidental cancellation between μ_F and μ_R dependence!

Scale variation (LHC @ 7 TeV, ATLAS setup, $p_{T,\gamma} > 15\,\mathrm{GeV}$)

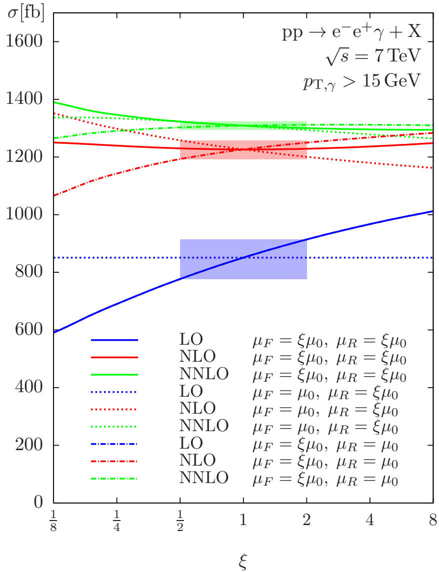

- (Central) scale choice:

  $\mu_R = \mu_F = \mu_0 \equiv \sqrt{m_Z^2 + p_{\gamma,T}^2}$.

- Scale variation essentially disappears at NLO and NNLO if variation with $\mu_F = \mu_R$ is considered.

  ↪ accidental cancellation between μ_F and μ_R dependence!

Scale variation (LHC @ 7 TeV, ATLAS setup, $p_{\mathrm{T},\gamma} > 15\,\mathrm{GeV}$)

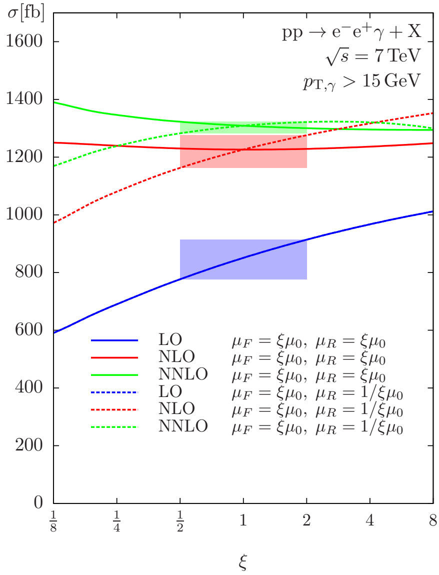

- (Central) scale choice:
  $\mu_\mathrm{R} = \mu_\mathrm{F} = \mu_0 \equiv \sqrt{m_\mathrm{Z}^2 + p_{\gamma,\mathrm{T}}^2}$.
- Scale variation essentially disappears at NLO and NNLO if variation with $\mu_\mathrm{F} = \mu_\mathrm{R}$ is considered.

  $\hookrightarrow$ accidental cancellation between μ_F and μ_R dependence!
- Solution: antipodal scale variation:
  $\mu_\mathrm{F} = \xi\mu_0,\ \mu_\mathrm{R} = 1/\xi\mu_0,\ \ \xi \in [0.5{,}2]$
  (also proposed by [Campbell, Ellis, Williams (2011)])

Resulting scale variation
($\mu_\mathrm{R},\ \mu_\mathrm{F} \in [0.5\mu_0, 2\mu_0]$) :

LO	NLO	NNLO
+7% −9%	+4% −5%	+1% −2%

Scale variation (LHC @ 7 TeV, ATLAS setup, $p_{\mathrm{T},\gamma} > 40\,\mathrm{GeV}$)

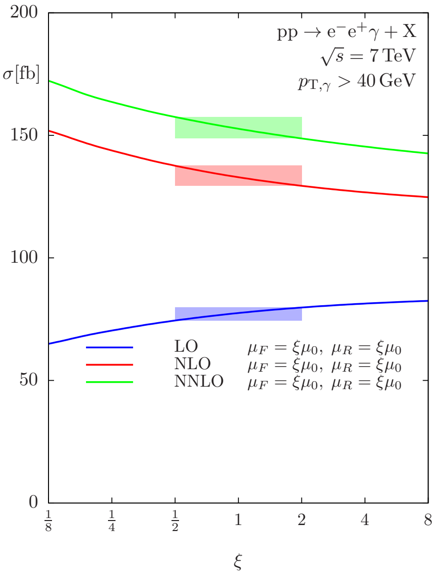

- Due to higher cut on $p_{\mathrm{T},\gamma}$, higher CMS energies (thereby higher x_1, x_2) involved.
  - Cross-section dependence on μ_F decreases (wrt. to lower $p_{\mathrm{T},\gamma}$ cut).
  - No significant cancellation between μ_F and μ_R dependence.
  - μ_R dominates scale dependence.
- Consider independent variations of μ_F and μ_R and take the envelope.

Resulting scale variation ($\mu_\mathrm{R},\ \mu_\mathrm{F} \in [0.5\mu_0, 2\mu_0]$) :

LO	NLO	NNLO
$+3\%$ -4%	$+4\%$ -4%	$+3\%$ -3%

Scale variation (LHC @ 7 TeV, ATLAS setup, $p_{\mathrm{T},\gamma} > 40\,\mathrm{GeV}$)

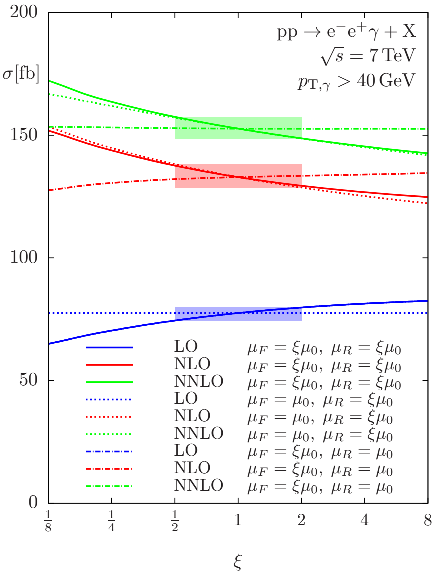

- Due to higher cut on $p_{\mathrm{T},\gamma}$, higher CMS energies (thereby higher x_1, x_2) involved.
  - Cross-section dependence on μ_F decreases (wrt. to lower $p_{\mathrm{T},\gamma}$ cut).
  - No significant cancellation between μ_F and μ_R dependence.
  - μ_R dominates scale dependence.
- Consider independent variations of μ_F and μ_R and take the envelope.

Resulting scale variation ($\mu_\mathrm{R},\ \mu_\mathrm{F} \in [0.5\mu_0, 2\mu_0]$) :

LO	NLO	NNLO
$+3\%$ -4%	$+4\%$ -4%	$+3\%$ -3%

Scale variation (LHC @ 7 TeV, ATLAS setup, $p_{\mathrm{T},\gamma} > 40\,\mathrm{GeV}$)

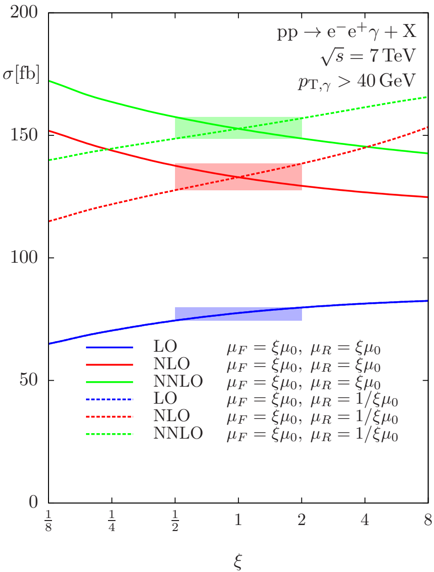

- Due to higher cut on $p_{\mathrm{T},\gamma}$, higher CMS energies (thereby higher x_1, x_2) involved.
  - Cross-section dependence on μ_{F} decreases (wrt. to lower $p_{\mathrm{T},\gamma}$ cut).
  - No significant cancellation between μ_{F} and μ_{R} dependence.
  - μ_{R} dominates scale dependence.
- Consider independent variations of μ_{F} and μ_{R} and take the envelope.

Resulting scale variation ($\mu_{\mathrm{R}},\ \mu_{\mathrm{F}} \in [0.5\mu_0, 2\mu_0]$) :

LO	NLO	NNLO
$^{+3\%}_{-4\%}$	$^{+4\%}_{-4\%}$	$^{+3\%}_{-3\%}$

NLO QCD cross section via dipole subtraction

Schematic formula for the NLO cross section with dipoles [Catani, Seymour (1993)]:

$$\sigma^{\text{NLO}} = \underbrace{\int_{m+1} d\sigma^R}_{\text{real corrections}} + \underbrace{\int_m d\sigma^V}_{\text{virtual corrections}} + \underbrace{\int_0^1 dz \int_m d\sigma^C}_{\text{collinear-subtraction counterterm}} - \int_{m+1} d\sigma^A + \int_{m+1} d\sigma^A,$$

$$d\sigma^A = \sum_{\text{dipoles}} d\sigma^B \otimes dV_{\text{dipole}}$$

$$= \int_{m+1} \left[d\sigma^R - d\sigma^A \right]_{\epsilon=0} \qquad \Rightarrow \text{RA}$$

$$+ \int_m \left[d\sigma^V + \sum_{\text{dipoles}} d\sigma^B \otimes V_{\text{dipole}}(1) \right]_{\epsilon=0} \qquad \Rightarrow \text{VA}$$

$$+ \int_0^1 dz \int_m \left[d\sigma^C + \sum_{\text{dipoles}} \int_1 d\sigma^B(z) \otimes [dV_{\text{dipole}}(z)]_+ \right]_{\epsilon=0} \qquad \Rightarrow \text{CA}$$

$$dV_{\text{dipole}}(z) = [dV_{\text{dipole}}(z)]_+ + dV_{\text{dipole}}(1)\delta(1-z)$$

NLO QCD cross section via q_T subtraction

Schematic formula for the NLO cross section

$$\sigma^{\mathrm{NLO}} = \underbrace{\int_{m+1} d\sigma^R}_{\text{real}} + \underbrace{\int_m d\sigma^V}_{\text{virtual}} + \underbrace{\int_0^1 dz \int_m d\sigma^C}_{\text{collinear counterterm}}$$

$$= \int_{m+1} d\sigma^R \Big|_{q_\mathrm{T}/q > \mathrm{cut}_{q_\mathrm{T}/q}}$$

$\Rightarrow$ finite, but depends on $\mathrm{cut}_{q_\mathrm{T}/q}$

$$+ \underbrace{\int_{m+1} d\sigma^R \Big|_{q_\mathrm{T}/q \leq \mathrm{cut}_{q_\mathrm{T}/q}}}_{\substack{\text{approximated by results known} \\ \text{from } q_\mathrm{T} \text{ resummation}}} + \underbrace{\int_m d\sigma^V + \int_0^1 dz \int_m d\sigma^C}_{\substack{\text{identified with corresponding terms} \\ \text{in } q_\mathrm{T} \text{ resummation}}}$$

$$\approx \int_{m+1} d\sigma^R \Big|_{q_\mathrm{T}/q > \mathrm{cut}_{q_\mathrm{T}/q}} + \frac{\alpha_S}{\pi} \mathcal{H}^{F(1)} \otimes \sigma_{\mathrm{LO}}$$

- no $\mathrm{cut}_{q_\mathrm{T}/q}$ dependence,
- contains (finite) 1-loop part.

$$+ \frac{\alpha_S}{\pi} \int_{\mathrm{cut}_{q_\mathrm{T}/q}}^{\infty} d(q_\mathrm{T}/q) \Sigma^{(1)}(q_\mathrm{T}/q) \otimes \sigma_{\mathrm{LO}}$$

- cancels $\mathrm{cut}_{q_\mathrm{T}/q}$ dependence,
- assigned to Born phase-space.